ARTICLES
https://doi.org/10.1038/s41558-019-0608-4
nature climate change

Sea-level-rise-induced threats depend on the size of tide-influenced estuaries worldwide

Jasper R. F. W. Leuven[1*], Harm Jan Pierik[1], Maarten van der Vegt[1], Tjeerd J. Bouma[1,2] and Maarten G. Kleinhans[1]

The effects of sea-level rise on the future morphological functioning of estuaries are largely unknown because tidal amplitudes will change due to combined deepening of the estuary mouth and shifting amphidromic points at sea. Fluvial sediment supply is also globally decreasing, which hampers infilling necessary to maintain elevation relative to sea level. Here we model 36 estuaries worldwide with varying sizes, shapes and hydrodynamic characteristics, and find that small shallow estuaries and large deep estuaries respond in opposite ways to sea-level rise. Large estuaries are threatened by sediment starvation and therefore loss of intertidal area, particularly if tidal amplitude decreases at the mouth. In contrast, small estuaries face enhanced flood risks and are more sensitive to tidal amplification on sea-level-rise-induced deepening. Estuary widening can partly mitigate adverse effects. In large estuaries, expanded intertidal areas increase tidal prism and available erodible sediment for adaptation, whereas it slightly reduces tidal amplification in small estuaries.

Estuaries are highly dynamic wetland zones at the transition from the river to the ocean, susceptible to future climate change and especially to sea-level rise (SLR)[1,2]. In estuaries such as the Western Scheldt, Elbe and Yangtze, the channels provide access to inland harbours[3] and the intertidal bars form a valuable ecological habitat[4]. The surrounding land is often densely populated; in fact, 21 of the world's 30 largest cities are located next to estuaries[5]. Potential SLR-induced threats are increased flood risk[6,7], reduced navigability[8] and drowning of the intertidal habitat area[3,9–12]. Estuary size and shape may affect their future response to SLR[13,14], but SLR-induced changes in morphology have so far received little attention. Here we study changes in morphology and the resulting tidal dynamics for estuaries of different sizes worldwide.

Estuarine bars, tidal flats and salt marshes have the potential to grow with SLR if they import sufficient fluvial or marine sediment to adapt the morphology to the new boundary conditions[15]. Three key boundary conditions for estuary morphology and their potential to adapt are (1) planform shape, (2) tidal amplitude at the estuary mouth and (3) sediment supply. Together these parameters control the overall volume of water (tidal prism) and sediment moving in and out of the estuary[14,16,17], which determine channel volume and the space available to form intertidal bars[18]. However, under SLR, tidal amplitudes at estuary mouths are likely to change because of shifting amphidromic points[19,20]. If the distance between the estuary mouth and amphidromic point increases, the tidal amplitude increases and vice versa. It remains unknown how the combined future SLR and changes in tidal amplitude will affect the tidal propagation and equilibrium morphology of bar-filled estuaries worldwide. Their future equilibrium morphology determines whether present-day fluvial sediment supply could be sufficient for adaptation of the morphology.

The balance between bed friction and channel-width convergence determines whether the tidal range amplifies (becomes larger), remains constant (an 'ideal estuary') or dampens (becomes smaller) in the landward direction[14,21–24]. A future increase in mean sea level (MSL) reduces bed friction, which means that the tidal range can become increasingly amplified. The consequence is flood risk (higher high waters) and reduced navigability (lower low waters).

Human exploitation has largely affected the natural processes occurring in deltas and estuaries in the past centuries[25]. In particular, dyke construction and land reclamation[3] have cut off the ecologically valuable flanking mudflats and salt marshes from the channels that supply sand and mud during inundations[26,27]. These intertidal areas provide storage space and friction for the tidal wave[21], thereby naturally reducing flood risk. However, the channels are dredged for harbour accessibility, which reduces friction for the tidal wave, thereby enhancing flood risk[3,10,11]. Additionally, dam construction in rivers has largely reduced fluvial sediment supply to estuaries[28–30]. Here we evaluate how flood risk and drowning threats can be mitigated by managed realignment. Managed realignment[31] means removing coastal protection to expose additional, currently terrestrial, areas to tidal flooding, which widens the estuary.

We calculate the morphological and hydrodynamic response of 36 estuaries worldwide to SLR and assess the potential for increased space by managed realignment. Estuaries varied from very small to very large (0.1–1,000 km^2), which allowed us to test the effect of estuary size on SLR-induced threats. The required sediment for adaptation and flood water levels within the estuary are used as main indicators for coping with SLR.

Approach and scenarios

The effect of future SLR was studied in three scenarios (Fig. 1). To do so, a semi-empirical morphological tool[32] was coupled with a one-dimensional (1D)-hydrodynamic model (see Methods) to estimate the present-day situation and the scenario effect. Here we briefly summarize the approach.

Depth distribution was estimated based on the estuary planform shape, tidal amplitude at the mouth and river discharge (Supplementary Fig. 4 and Supplementary Table 2). Average depth at the landward boundary and seaward boundary were obtained from hydraulic geometry relations that were developed for rivers

[1]Faculty of Geosciences, Utrecht University, Utrecht, the Netherlands. [2]Royal Netherlands Institute for Sea Research, Yerseke, the Netherlands.
*e-mail: j.r.f.w.leuven@uu.nl

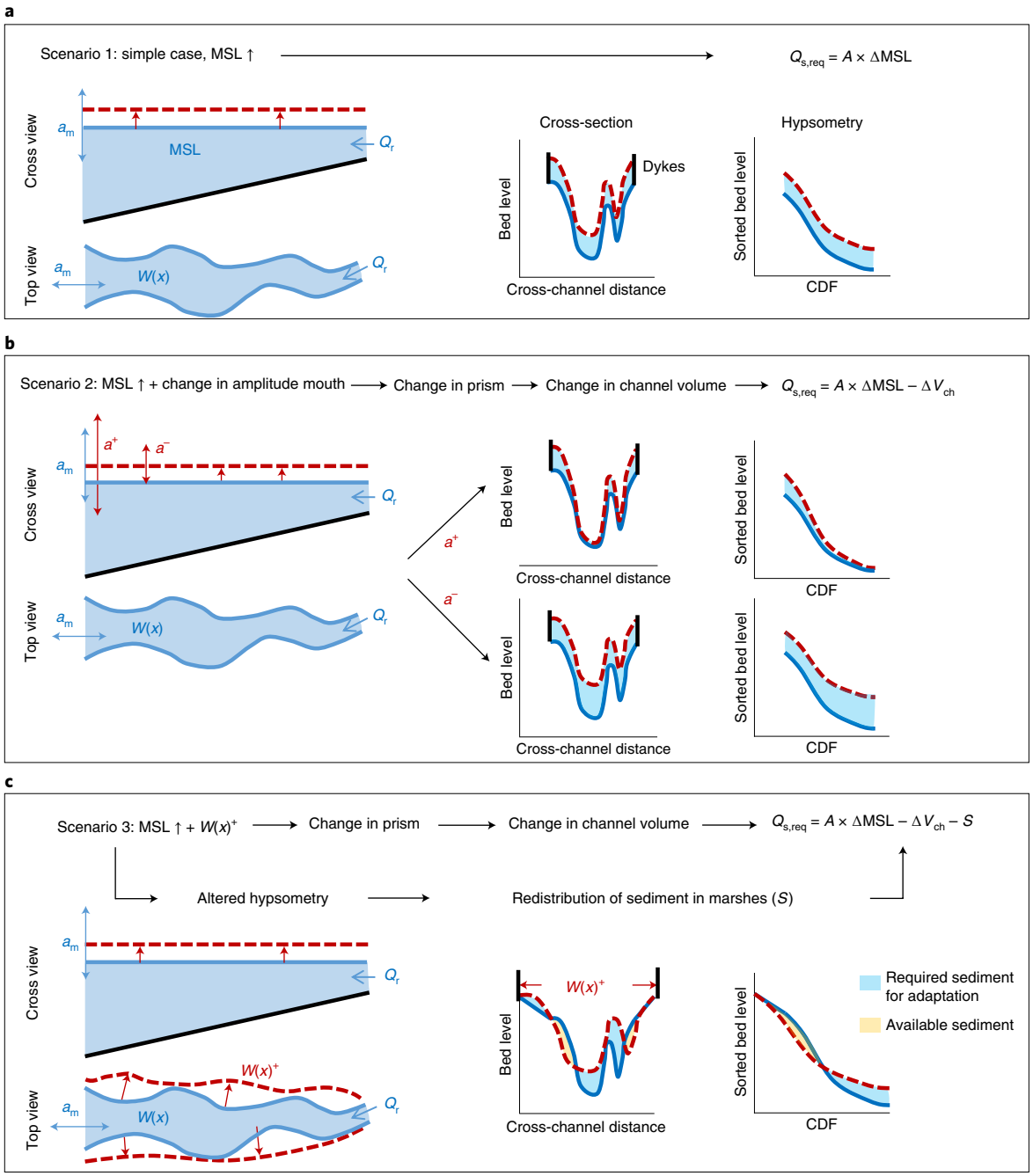

Fig. 1 | SLR effects on boundary conditions of estuaries. a–c, Flowcharts along the top of panels indicate main morphological effects. The red dashed line indicates the scenario effect on water level and estuary width. Red arrows indicate changes in tidal amplitude at the mouth; a_m, tidal range at the mouth; Q_r, river discharge. The cumulative distribution functions (CDFs) indicate hypsometric curves that summarize cross-sectional bed elevations in cumulative profiles. **a**, In the simple case (scenario 1, an increase in MSL), all boundary conditions remain equal, which means that the required sediment ($Q_{s,req}$) for adaptation is the estuary surface area (A) multiplied by the increase in MSL (ΔMSL). **b**, Tidal range either increases (scenario 2, a^+), decreases (scenario 2, a^-) or remains the same (scenario 1, a^0) depending on the location of the estuary in relation to its amphidromic point (tidal node). Changes in tidal amplitude at the mouth modify the tidal prism and thereby alter the equilibrium channel volume (V_{ch}). This increases the required sediment for adaptation for decreasing amplitude (a^-) and decreases the required sediment for increasing tidal amplitude (a^+). **c**, The estuary widens (scenario 3, $W(x)^+$) if surrounding land is drowned or by managed realignment. Increased planform width ($W(x)$) has a similar effect as scenario 2, but it additionally alters the cross-sectional distribution of bed levels, which means that salt marsh sediments become available for redistribution.

and estuaries of different size and character[17,33–35]. Subsequently, the cross-sectional distribution of bed levels (that is, the hypsometry) was obtained from a morphological relation between the local width and the width as expected from a fitted converging shape (ideal[17,18,22,36,37]). This relation results in a wide intertidal area when the local estuary is relatively large and vice versa for relatively narrow sections. The morphological output was translated into 1D-profiles of channel width, average channel depth, shoal width and average

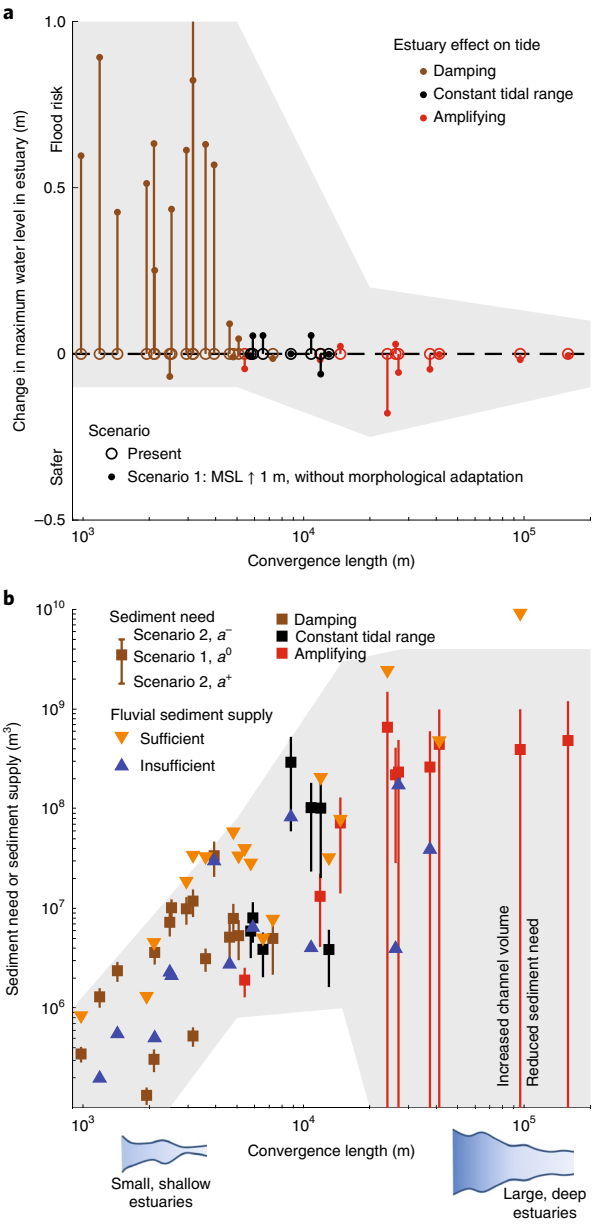

Fig. 2 | Estuary size dependency on SLR-induced threats. a, Possible trajectories of SLR-induced changes in maximum water level within the estuary against convergence length, which is a measure of estuary size. Lines indicate the effect of 1-m SLR without morphological adaptation (scenario 1). Shallow damping estuaries are probably most sensitive to future increases in water level and impose a flood risk, while deep amplifying estuaries are insensitive. **b**, Sediment need or sediment supply for adaptation with 1-m SLR over a period of 100 years against estuary convergence length. Vertical lines indicate the sensitivity to increased (scenario 2, a^+) or decreased (scenario 2, a^-) tidal amplitude. Squares indicate the required sediment when amplitude at the mouth remains constant; triangles indicate estimated fluvial sediment supply over 100 years. Blue triangles indicate a sediment supply less than the requirement under the a^0 scenario. Orange triangles indicate a surplus of fluvial sediment input. Large amplifying estuaries are very sensitive to changes in tidal amplitude on required sediment for adaptation, while small damping estuaries are less sensitive. Large estuaries with increasing tidal amplitude have sufficient sediment input from the river for adaptation, while a decrease in tidal amplitude would lead to a larger requirement than supplied by the river. The grey shaded area indicates the generalized effect of estuary size on future water levels and sediment need.

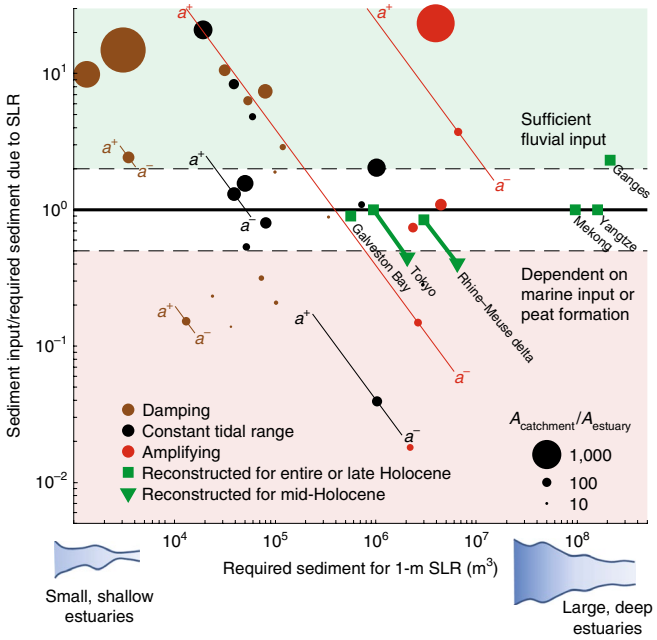

Fig. 3 | Relative upstream sediment input from the catchment versus the range of required sediment for 1-m SLR depending on the change of tidal amplitude. Required sediment is an indicator for estuary size when all boundary conditions remain constant (scenario 1). Rivers with a relatively large catchment area ($A_{catchment}$) compared to estuary area ($A_{estuary}$) deliver sufficient sediment to estuaries, which can therefore adapt to rising sea level, while other estuaries may depend on marine sediment input, peat formation or sediment nourishment for morphological adaptation. The sensitivity to changes in tidal amplitude (see Fig. 2) are indicated for a small selection of all systems indicated in Fig. 2. Holocene sediment budgets from geological cases are added as a reference for minimal sediment supply potential. Mid-Holocene cases experienced SLR comparable to future SLR (see also Supplementary Table 1).

shoal depth, which were used for a 1D-hydrodynamic model that solves the shallow water equations, resulting in the tidal range along the estuary[21]. This along-channel tidal range was used as the main indicator for flood safety, navigability and intertidal habitat area.

The three SLR scenarios increase in complexity. Scenario 1 is a worst-case increase in MSL of 1 m in 100 years and was used to analyse the effect of increased channel depth on tidal amplification (Fig. 1)[1,14,19,27]. Scenario 1 provides a baseline for the required sediment volume. Because all boundary conditions that affect morphology remain constant, the future morphology is assumed to adapt so much slower than the sea level rises that it remains effectively equal to the estimated present-day morphology. The sudden deepening leads to flood-dominant estuaries that tend to import available sediment. This means that the required sediment demand for recovering morphological equilibrium at a higher sea level is simply the estuary surface area multiplied by the increase in MSL (Fig. 1a). In reality, however, the required sediment is modified by changes in tidal amplitude at the mouth due to SLR-imposed shifts of amphidromic points[19,20], which means the estuary has to adapt to a new equilibrium. Scenario 2 therefore explores the effect of changes in tidal amplitude at the mouth, varying from a decrease of 0.25 m (a^-) up to an increase of 0.50 m (a^{++}) (Fig. 1b). This scenario illustrates the effect of future changes in tidal amplitude at the mouth on the required sediment for adaptation. In scenarios 1 and 2, the estuary width was assumed to remain constant (we assume barriers such as embankments that prevent any surrounding land from flooding); however, in scenario 3 the effect of increased

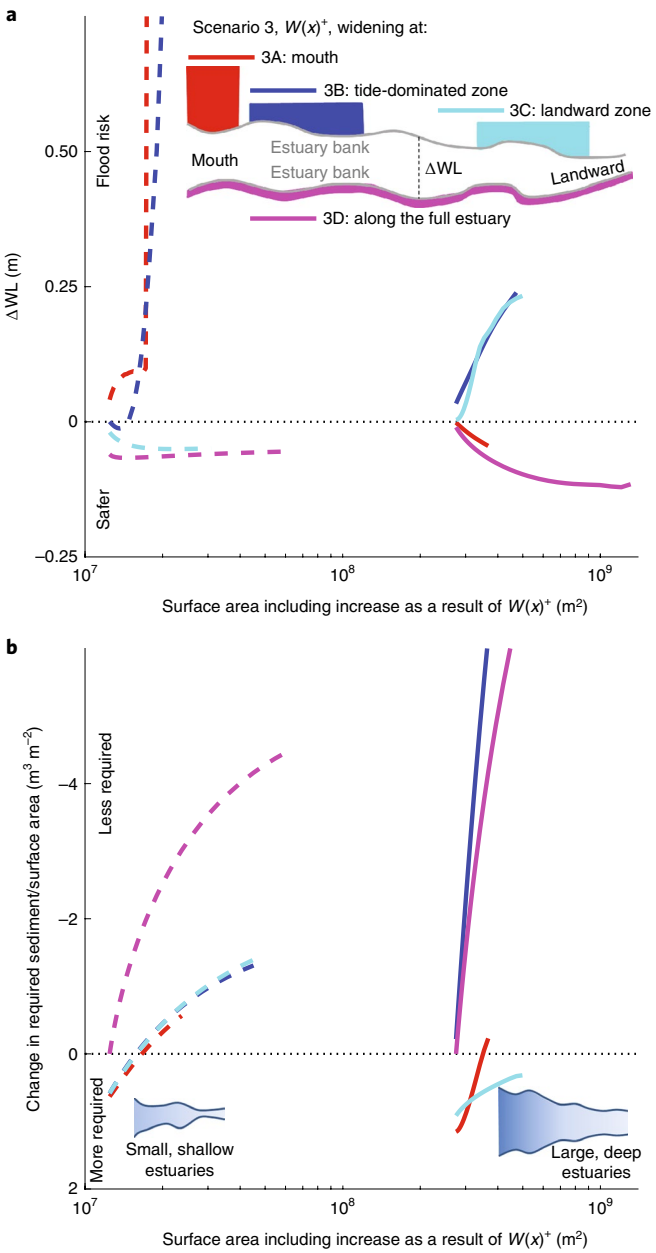

Fig. 4 | Effects of managed realignment. a,**b**, Change in water level within the estuary (ΔWL, **a**) and change in required sediment for adaptation normalized by surface area plotted against degree of estuary widening (**b**). Dashed lines indicate idealized model results for scenarios 3A–D for a small estuary (length of 15 km) and solid lines indicate a large estuary (length of 70 km). Widening was implemented on a fixed length and thus with variable local width. The type of widening in scenario 3 has a large effect on required sediment for large estuaries and on water levels in small estuaries. Increased estuary width increases tidal prism at the mouth, but only when the widening is located seaward of the tidal excursion length, which is the distance a particle of water travels in half a tidal cycle. Increased tidal prism increases channel depth and volume, and therefore reduces required sediment. However, increased depth also reduces friction, which increases water levels in the estuary.

estuary width is investigated (Fig. 1c). The increased estuary width modifies the estimated equilibrium morphology. Furthermore, sediment from former, flooded salt marshes becomes partly available for redistribution.

Scenario 1 is predominantly used to study the effect of increased channel depth on tidal amplification. Scenario 2 reveals a relation between required sediment for adaptation and future changes in tidal range. Scenario 3 explains under which conditions managed realignment has the potential to mitigate adverse effects of the previous scenarios. Furthermore, the results of sediment requirement were compared with geological cases, serving as references for the fate of estuaries. For this we used past planform sizes of six systems (Supplementary Table 1), which had previously evolved under SLR, that were in the same order of the expected future SLR.

Estuary dimensions control the effects of SLR

We show that morphological and hydrological responses to SLR are different between small (channel convergence length $<10^4$ m), shallow (<10 m deep) and damping (hyposynchronous) estuaries and large (channel convergence length $>10^4$ m), deep (>10 m deep) and amplifying (hypersynchronous) estuaries (Fig. 2). Size dependency on responses to SLR was found in all three scenarios, for which the results are detailed below. Size-related characteristics (that is, the characteristic channel convergence length, depth of the estuary and present-day tidal prism) proved to be very strong indicators of sensitivity to SLR. Other estuary characteristics, for example an increase in tidal prism from a widened estuary planform and the ratio between bar area and total area, proved to be less suitable indicators for sensitivity to future SLR (Supplementary Fig. 5).

Future flood risk, navigability and intertidal area

We found that large estuaries, which in all cases show tidal amplification, are unlikely to amplify even more under SLR (scenario 1) even if they receive insufficient sediment to adapt to SLR (Fig. 2a). In contrast, small systems, which in all cases currently show tidal damping, respond extremely sensitively by having a large increase in tidal range (scenario 1, Fig. 2a). Small, and thus shallow, estuaries are typically friction-dominated. For these estuaries, a 1-m increase in water depth results in a relatively large reduction in friction[21], which causes tidal amplification. Scenarios applied in a 1D-hydrodynamic model suggest that small estuaries, when drowning, would have maximum water levels in the estuary increased by 0.3–0.8 m on top of the increase in MSL, which is predominantly due to reduction of friction. In contrast, friction in relatively large, and thus deep, estuaries is much less, which means that the same increase in MSL has a smaller effect on tidal amplification (Fig. 2a).

The changes related to estuary size provide opportunities and challenges for human use and ecosystem services. If tidal amplitude increases within the estuary, navigability during low tide will be reduced and flood risk during high water will be increased. However, the outcomes for navigability and flood safety are upper limit estimates because scenario 1 excludes morphological adaptation, changes in tidal amplitude at the mouth and the effects of increased mean water levels that occur during storm surges (see Supplementary Text).

Tidal amplification (a possible result of scenario 1) and SLR in combination with changes in tidal amplitude at the mouth (scenario 2) cause intertidal areas to change in multiple ways, depending on estuary size and sediment supply. First, a change in the tidal amplitude boundary condition (scenario 2) directly affects the intertidal area, which includes pioneering salt marshes[12,38], by increasing or decreasing the range of bed levels that inundate and drain over a tidal cycle. Although increased tidal amplitude deepens the estuary and increases channel volume, the highest areas of the marshes and the subtidal areas of bars are transformed into intertidal areas due to the increased tidal range[32]. Second, tidal amplification (scenario 1) increases the tidal range in the landward direction, which could result in an increased intertidal area in the landward direction for the same reason.

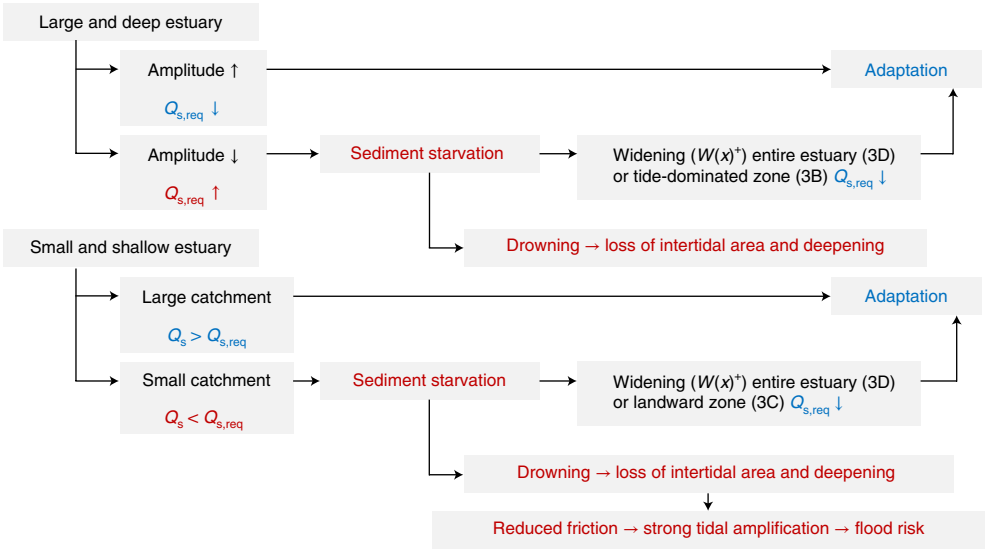

Fig. 5 | Main responses of estuaries to SLR. Large, deep, amplifying estuaries are susceptible to sediment starvation if tidal amplitude at the mouth decreases. This can be counteracted by increased space for the estuary along the entire channel, which could increase tidal prism and available erodible sediment for adaptation, or in the tide-dominated zone at the expense of higher water levels in the estuary. Small, shallow, damping estuaries are susceptible to future tidal amplification when sediment supply is insufficient to adapt the morphology to SLR. Managed realignment can potentially reduce amplification, but only when it is implemented in the most landward part of the estuary or along the entire estuary (Fig. 4). The benefit of the latter is that it also strongly decreases the required sediment for adaptation. Blue (red) text and symbols represent positive (negative) effects.

Present results thus illustrate how two opposing threats and values may compete in the future: increased tidal amplitudes could increase flood risk during high waters and reduce navigability during low tides, but increase valuable intertidal habitat area, and vice versa for reduced tidal amplitude. The potential morphological adaptation of channels, bars and intertidal areas under SLR depends mainly on the required sediment input, which is discussed next.

Importance of sediment balance

A comparison of present fluvial sediment supply[39] and required sediment for adaptation to a possible new equilibrium state (scenario 2) shows that most large estuaries may have sufficient fluvial input if tidal amplitude at the mouth increases, but that they probably have a shortage if tidal amplitude decreases (Fig. 2b). This surprising result is caused by the increase in channel volume with tidal prism (scenario 2, a^+ and a^{++}), which partly compensates for the required sediment due to an increase in MSL (scenario 1) (Supplementary Fig. 6a). A decrease in tidal amplitude (scenario 2, a^-), on the other hand, requires much more sediment (Fig. 2b) to follow SLR because it reduces the equilibrium depth and volume of channels (Fig. 1).

The morphological response and dependency on sediment supply to scenarios 2 is different for large and small estuaries. Large estuaries with relatively deep channels and a weak channel convergence show a strong morphological response to changes in tidal amplitude by relatively large changes in channel volume (Fig. 2b). Geological examples are the Rhine–Meuse Delta and Tokyo Bay that drowned in the mid-Holocene (Fig. 3). Over the entire Holocene, drowning was eventually compensated for, indicating that it took thousands of years of major sediment supply under stabilizing sea levels to compensate for this drowning. The Ganges is an example of how excessive amounts of sediment supply over the Holocene not only compensates for SLR, but even causes delta progradation.

In contrast, small estuaries are much less sensitive to changes in tidal amplitude at the mouth (Fig. 2b) because the change in tidal prism by amplitude change depends mainly on basin surface area. This means that small estuaries are not easily starved of sediment when tidal amplitude at the mouth reduces, but they also do not compensate for SLR in case of increased amplitude at the mouth. Whether small estuaries adapt depends mainly on the current supply of fluvial and coastal sediment compared to the estuary size.

Our results indicate that estuaries with a larger ratio of catchment area to estuary area are more likely to receive sufficient fluvial input than estuaries with relatively small catchments (Fig. 3). Here we showed that estuaries that are relatively large compared to the catchment area are sensitive to drowning, but that this effect can be counteracted by increased tidal amplitude at the mouth. In general, it is expected that drowning estuaries become more flood-dominant[40,41] and thereby import more sediment, provided that sediment is available. The actual sediment need on sediment-rich coasts may thus be lower than estimated, which means that our estimates are at the upper limit.

The possible SLR-induced responses and controlling factors in this study may serve as a guideline for more focused studies on the process–response dynamics in individual case studies. A worldwide analysis and the lack of bathymetric data required us to simplify our approach to obtain upper and lower limit estimates of the system-scale effects. Further development of data-dependent models is needed for individual estuaries to include process–response dynamics (coupled hydrodynamic–morphological models). The present modelling assumed the highly disequilibrium response to SLR, but for faster morphological response and slower SLR scenarios coupled modelling between SLR, tidal asymmetry and the resulting net sediment transport that determine morphological adaptation is required (for example, Wang et al.[40,41]). The results in this study provide a frame of reference and estimation of trajectories for estuaries of different size and character.

Implications for mitigation

Modelling scenario 3 shows that managed realignment (that is, local floodplain widening) has the potential to counteract sediment starvation in large estuaries and increase flood risk slightly in small estuaries. For example, the model results suggest a maximum reduction of 10 cm in flood water levels in small estuaries (Fig. 4a), which is only 10% compared to flood water levels that may increase by up to 1 m on top of the increase in MSL (Fig. 2a). In small estuaries, widening in the landward zone (zone 3C in Fig. 4a) or along the

entire estuary (zone 3D) was found to be most effective at reducing water levels in the estuary (Fig. 4a). This results in wider tidal flats that enhance tidal damping (Fig. 4). The latter (zone 3D) also has a strong positive effect on the sediment balance (Fig. 4b). If the extra sediment available from the widened areas is sufficient for the estuary to adapt, the effect of increased water depth on tidal amplification is also mitigated. Keeping dredged sediment in the system for future availability, rather than extraction, may therefore also be needed. Widening at the mouth (zone 3A) or in the tide-dominated zone (zone 3B) are not recommended because widening at the mouth (zone 3A) may increase the channel width along the estuary, while widening in the tidal zone (zone 3B) increases tidal prism and therefore deepens channels in the tide-dominated zone, which outweighs the positive effects of increased shoal area.

For large estuaries, managed realignment (scenario 3) is most effective when implemented along the entire estuary (Fig. 4, zone 3D). Widening in the tide-dominated zone (zone 3B) is also effective for the sediment balance, but at the cost of increased water levels (Fig. 4a). Generally, if the estuary is widened close enough to the mouth to be able to affect the tidal prism, channels may enlarge and therefore less sediment is required for adaptation. Widening also alters the bed level estimations per cross-section (that is, the hypsometric curve), which may result in erosion and reworking of sediment from former salt marshes.

If the natural sediment supply is too low for natural adaptation, management options may provide alternative adaptation pathways[42,43]. These options include sediment nourishment on the ebb-tidal delta to increase sediment import from the sea[44] or estuary widening by managed realignment (scenario 3). Our results show that widening, with breakdown and reworking of salt marshes on sandy substrates, would deliver part of the sediment required for adaptation to SLR, but at the cost of intertidal and supratidal habitat. Moreover, local widening would increase accommodation space, which was recently found to stimulate the resilience of global wetlands because it allowed them to grow vertically by sediment accretion[27]. We therefore conclude that managed realignment is an important measure to implement before potential dyke breaching leads to land loss in densely populated areas.

Conclusions

Here we present a range of SLR-induced responses that depend on estuary dimensions. We found that large and deep systems may face sediment starvation, particularly when tidal amplitude decreases (Fig. 5). Large systems are relatively sensitive to changes in sediment supply required for adaptation. This is the case because future changes in tidal prism are influenced by a combination of tidal amplitude and basin surface area, and basin surface area is relatively large in these systems. The effects of changes in tidal amplitude at the mouth on necessary sediment volumes are therefore expected to increase with system scale. In contrast, small and shallow estuaries are most sensitive to tidal amplification, potentially causing an increased flood risk (Fig. 5). These shallow estuaries are currently friction-dominated, which means that a 1-m increase in water depth may result in a relatively large reduction in friction, which typically leads to tidal amplification.

Allowing more space for flooding, for example by managed realignment, has the potential to reduce adverse changes. Increasing estuary width counteracts sediment starvation and increased water levels depending on location and subsoil composition. In large estuaries, this increases tidal prism and available erodible sediment for adaptation, whereas in small estuaries it enhances tidal damping (Fig. 5). The results in this study are promising for further assessment of changing estuary shape and changing tidal regimes. Our proposed SLR-induced responses and controlling factors can serve as a guideline for studies dedicated to the process–response dynamics of individual case studies.

Online content

Any methods, additional references, Nature Research reportingsummaries, source data, extended data, supplementary information,acknowledgements, peer review information; details of authorcontributions and competing interests; and statements of data andcode availability are available at https://doi.org/10.1038/s41558-019-0608-4.

Received: 8 February 2019; Accepted: 18 September 2019;
Published online: 4 November 2019

References

1. Church, J. A. et al. in *Climate Change 2013: The Physical Science Basis* (eds Stocker, T. F. et al.) 1137–1216 (IPCC, Cambridge Univ. Press, 2013).
2. Wong, P. P. et al. in *Climate Change 2014: Impacts, Adaptation, and Vulnerability* (eds Field, C. B. et al.) 361–409 (IPCC, Cambridge Univ. Press, 2014).
3. de Vriend, H. J., Wang, Z. B., Ysebaert, T., Herman, P. M. & Ding, P. Eco-morphological problems in the Yangtze Estuary and the Western Scheldt. *Wetlands* **31**, 1033–1042 (2011).
4. Bouma, H., de Jong, D. J., Twisk, F. & Wolfstein, K. *A Dutch Ecotope System for Coastal Waters (ZES. 1): To Map the Potential Occurence of Ecological Communities in Dutch Coastal and Transitional Waters* Technical Report No. RIKZ/2005.024 (Rijkswaterstaat, 2005).
5. Ashworth, P. J., Best, J. L. & Parsons, D. R. *Fluvial–Tidal Sedimentology* (Elsevier, 2015).
6. Nicholls, R. J. & Cazenave, A. Sea-level rise and its impact on coastal zones. *Science* **328**, 1517–1520 (2010).
7. Auerbach, L. W. et al. Flood risk of natural and embanked landscapes on the Ganges–Brahmaputra tidal delta plain. *Nat. Clim. Change* **5**, 153–157 (2015).
8. Mao, Q., Shi, P., Yin, K., Gan, J. & Qi, Y. Tides and tidal currents in the Pearl River Estuary. *Cont. Shelf Res.* **24**, 1797–1808 (2004).
9. Costanza, R. et al. The value of the world's ecosystem services and natural capital. *Nature* **387**, 253–260 (1997).
10. Essink, K. Ecological effects of dumping of dredged sediments; options for management. *J. Coast. Conserv.* **5**, 69–80 (1999).
11. Yuan, R. & Zhu, J. The effects of dredging on tidal range and saltwater intrusion in the Pearl River Estuary. *J. Coast. Res.* **31**, 1357–1362 (2015).
12. Balke, T., Stock, M., Jensen, K., Bouma, T. J. & Kleyer, M. A global analysis of the seaward salt marsh extent: the importance of tidal range. *Water Resour. Res.* **52**, 3775–3786 (2016).
13. Ensing, E., de Swart, H. E. & Schuttelaars, H. M. Sensitivity of tidal motion in well-mixed estuaries to cross-sectional shape, deepening and sea-level rise. *Ocean Dynam.* **65**, 933–950 (2015).
14. Du, J. et al. Tidal response to sea-level rise in different types of estuaries: the importance of length, bathymetry and geometry. *Geophys. Res. Lett.* **45**, 227–235 (2018).
15. Lentz, E. E. et al. Evaluation of dynamic coastal response to sea-level rise modifies inundation likelihood. *Nat. Clim. Change* **6**, 696–700 (2016).
16. Kirwan, M. L. & Guntenspergen, G. R. Influence of tidal range on the stability of coastal marshland. *J. Geophys. Res.* **115**, F02009 (2010).
17. Leuven, J. R. F. W., de Haas, T., Braat, L. & Kleinhans, M. G. Topographic forcing of tidal sand bar patterns for irregular estuary planforms. *Earth Surf. Process. Landf.* **43**, 172–186 (2018).
18. Leuven, J. R. F. W., Selaković, S. & Kleinhans, M. G. Morphology of bar-built estuaries: empirical relation between planform shape and depth distribution. *Earth Surf. Dyn.* **6**, 763–778 (2018).
19. Idier, D., Paris, F., Le Cozannet, G., Boulahya, F. & Dumas, F. Sea-level rise impacts on the tides of the european shelf. *Cont. Shelf Res.* **137**, 56–71 (2017).
20. Pickering, M. et al. The impact of future sea-level rise on the global tides. *Cont. Shelf Res.* **142**, 50–68 (2017).
21. Friedrichs, C. T. & Aubrey, D. G. Non-linear tidal distortion in shallow well-mixed estuaries: a synthesis. *Estuar. Coast. Shelf Sci.* **27**, 521–545 (1988).
22. Savenije, H. H. G. *Salinity and Tides in Alluvial Estuaries* (Elsevier, 2006).
23. Boelens, T., Schuttelaars, H., Schramkowski, G. & de Mulder, T. The effect of geometry and tidal forcing on hydrodynamics and net sediment transport in semi-enclosed tidal basins. *Ocean Dyn.* **68**, 1285–1309 (2018).
24. Silvestri, S., D'Alpaos, A., Nordio, G. & Carniello, L. Anthropogenic modifications can significantly influence the local mean sea level and affect the survival of salt marshes in shallow tidal systems. *J. Geophys. Res. Earth Surf.* **123**, 996–1012 (2018).
25. Temmerman, S. & Kirwan, M. L. Building land with a rising sea. *Science* **349**, 588–589 (2015).
26. Kirwan, M. L. & Megonigal, J. P. Tidal wetland stability in the face of human impacts and sea-level rise. *Nature* **504**, 53–60 (2013).
27. Schuerch, M. et al. Future response of global coastal wetlands to sea-level rise. *Nature* **561**, 231–234 (2018).

28. Walling, D. E. & Fang, D. Recent trends in the suspended sediment loads of the world's rivers. *Glob. Planet. Change* **39**, 111–126 (2003).
29. Yang, S. L. et al. Impact of dams on Yangtze River sediment supply to the sea and delta intertidal wetland response. *J. Geophys. Res.* **110**, F03006 (2005).
30. Dunn, F. E. et al. Projections of declining fluvial sediment delivery to major deltas worldwide in response to climate change and anthropogenic stress. *Environ. Res. Lett.* **14**, 084034 (2019).
31. Turner, R. K., Burgess, D., Hadley, D., Coombes, E. & Jackson, N. A cost–benefit appraisal of coastal managed realignment policy. *Glob. Environ. Change* **17**, 397–407 (2007).
32. Leuven, J. R. F. W., Verhoeve, S., van Dijk, W. M., Selaković, S. & Kleinhans, M. G. Empirical assessment tool for bathymetry, flow velocity and salinity in estuaries based on tidal amplitude and remotely-sensed imagery. *Remote Sens.* **10**, 1915 (2018).
33. Jarrett, J. T. *Tidal Prism: Inlet Area Relationships* Technical Report No. WES-GITI-3 (US Army Engineer Waterways Experiment Station, 1976).
34. Eysink, W. D. Morphologic response of tidal basins to changes. *Coast. Eng. Proc.* **22**, 1948–1961 (1990).
35. Gisen, J. I. A. & Savenije, H. H. G. Estimating bankfull discharge and depth in ungauged estuaries. *Water Resour. Res.* **51**, 2298–2316 (2015).
36. Langbein, W. The hydraulic geometry of a shallow estuary. *Hydrol. Sci. J.* **8**, 84–94 (1963).
37. Dronkers, J. Convergence of estuarine channels. *Cont. Shelf Res.* **144**, 120–133 (2017).
38. Kirwan, M. L., Walters, D. C., Reay, W. G. & Carr, J. A. Sea-level driven marsh expansion in a coupled model of marsh erosion and migration. *Geophys. Res. Lett.* **43**, 4366–4373 (2016).
39. Milliman, J. D. & Syvitski, J. P. Geomorphic/tectonic control of sediment discharge to the ocean: the importance of small mountainous rivers. *J. Geol.* **100**, 525–544 (1992).
40. Wang, Z. B., Jeuken, M.-C. J. L., Gerritsen, H., de Vriend, H. J. & Kornman, B. A. Morphology and asymmetry of the vertical tide in the Westerschelde estuary. *Cont. Shelf Res.* **22**, 2599–2609 (2002).
41. Friedrichs, C. T. in *Contemporary Issues in Estuarine Physics* (ed. Valle-Levinson, A.) 27–61 (Cambridge Univ. Press, 2010).
42. Kwadijk, J. C. J. et al. Using adaptation tipping points to prepare for climate change and sea-level rise: a case study in the Netherlands. WIREs. *Clim. Change* **1**, 729–740 (2010).
43. Haasnoot, M., Kwakkel, J. H., Walker, W. E. & ter Maat, J. Dynamic adaptive policy pathways: a method for crafting robust decisions for a deeply uncertain world. *Glob. Environ. Change* **23**, 485–498 (2013).
44. Wang, Z. B., Elias, E. P., van der Spek, A. J. & Lodder, Q. J. Sediment budget and morphological development of the Dutch Wadden Sea: impact of accelerated sea-level rise and subsidence until 2100. *Neth. J. Geosci.* **97**, 183–214 (2018).

Methods

The following steps were taken. First, estuary planforms where collected using Google Earth along with the present-day tidal range at the mouth and river discharge at the upstream boundary (Supplementary Table 2). Second, an empirical assessment tool was used to estimate the present-day and future equilibrium morphology of these estuaries[32]. Third, the output morphology served as input to a 1D-hydrodynamic model[21], which was used to study tidal amplification and damping. We applied three SLR scenarios to study the effect on morphology and tidal amplification. Finally, the required sediment for morphological adaptation under SLR was compared with the present-day sediment input to estuaries and reconstructions of former coastal systems under SLR.

To perform a worldwide analysis, we estimated the equilibrium morphology using empirical relations rather than coupled hydrodynamic–morphological models. Although the latter type of models are powerful tools, they are unsuitable for performing a worldwide analysis on estuaries due to their time consumption and the lack of data to initiate them. In our previous work[17,18,32] we validated our methods and estimated any associated uncertainties. In the Supplementary Information and Supplementary Fig. 3 how these uncertainties affect the main results in this study: that is, modelled flood water levels and required sediment for adaptation. The resulting uncertainty was a maximum of about 0.1 m for flood water levels and a factor of 1.5 for required sediment for adaptation (Supplementary Fig. 3).

Data collection of estuary planforms. An existing dataset with estuary planforms[17] was used and enhanced for this study. The dataset consists of 36 bar-filled estuaries worldwide of varying size, degree of tidal influence, river discharge and human influence (Supplementary Table 2). Channel planform was visually recorded using Google Earth due to a lack of sufficient detailed bathymetries. Google Earth uses a combination of space shuttle imagery, satellite imagery and aerial photography. Image resolution therefore varies from 30 m in Landsat imagery when completely zoomed out, up to 0.15 m for local aerial photography when zoomed in on the system scale or smaller. Channel planforms were recorded in this study at resolutions of at least 5 m, which is sufficient to capture the variations in planform and width.

For each estuary, the present-day planform was recorded. The tidal range at the mouth and river discharge were obtained from the datasets reported in Leuven et al.[17,45]. The present-day planform covers the part of the estuary in which large (>100 m) dynamic channels and bars occur and is approximately the area submerged at high tide level. This means that we exclude those parts of the high marsh that do not flood daily, similar to other higher elevated areas surrounding the estuary. The presence of dense vegetation is a good indicator of an area that is not flooded on a daily basis because an inundation duration of more than 50% time often inhibits vegetation growth and most vegetation settles permanently above the mean high tide level.

We tested the sensitivity of the 1D-hydrodynamic model results to erroneous estimates of the salt marsh area by including salt marshes equal to 20% of the local estuary width along the entire estuary. Our model showed that this affected water levels by less than 5% of the reported values. This implies that addition of salt marshes above the high tide level has a limited effect on the main conclusions of our research.

Tool for equilibrium morphology of estuaries. The along-channel width profile, tidal range at the seaward mouth of the estuary and river discharge were used for the empirical assessment tool that estimates equilibrium morphology[32] (Supplementary Fig. 1). The tool estimates the tidal prism at the mouth based on surface area and tidal range. The tidal prism is used to estimate the maximum and average depth at the mouth from a classic stability relation[33–35]. Similarly, a hydraulic geometry relation is applied at the landward boundary to obtain depth from river discharge. Together, these boundary conditions result in an along-channel maximum depth profile. Although the exact relation between tidal prism and the cross-sectional area is based on a slight misprediction of the tidal prism, these relations still capture the SLR-induced effects on cross-sectional area. The distribution of bed levels per cross-section (the hypsometry) depends on the ratio between the local width and the width as expected from a fitted converging shape (ideal[17,18,22,36,37]). We estimate hypsometry to be convex with a wide zone of intertidal area at locations where the estuary is wide relative to the fitted convergent channel; however, a more concave hypsometry with narrow stretches of intertidal area is expected at locations where the estuary width is close to the ideal width profile.

This simplified approach to estimating tidal prism neglects the amplification and damping of the tide as well as changes in the character of wave (standing versus propagating character). This means that for small and damping estuaries we might overestimate the tidal prism, and for large and amplifying estuaries we might underestimate the tidal prism by 10–40%. However, this simplification has a limited effect on the results in this study. If we overestimate tidal prism for small estuaries, it also means that we overestimate their depth. If their depth is indeed smaller, this could lead to larger friction and therefore an even larger sensitivity of future water levels to SLR. For large estuaries, the opposite reasoning holds. The depth boundary conditions can, in principle, be derived from data but were estimated in this study, pending future bathymetric data collection.

1D-hydrodynamic model. To investigate the degree of tidal amplification (flood water levels) or damping within estuaries we ran a number of model scenarios. We used a 1D-hydrodynamic model that has been demonstrated to reproduce important tidal dynamics[41] (Supplementary Figs. 2 and 4, and see Code availability). The model solves the shallow water equations (differential equations that describe fluid flow), excluding the effects of advection, with momentum transported solely through a rectangular channel. The continuity equation incorporates a linearly sloping intertidal area to allow width variation with water level and thereby simulates storage of water on the intertidal flats. For each estuary, the tidal range and depth at the estuary mouth were taken directly from the tool[32]. Along the estuaries, the cross-sectional hypsometry was divided into a channel part and a shoal part at the low water level, which is how we defined channel width. Subsequently, the average channel depth, channel width, shoal gradient and shoal width were calculated per cross-section. The linear cross-channel shoal gradient was calculated such that the storage volume is equal to the storage volume that results from the hypsometry above the low water line. Along-channel profiles of these characteristics were used as input to the model. The spatial step varied between 50 and 500 m, depending on the size of the estuary, and the time step was adjusted accordingly based on the Courant number.

Roughness was implemented as follows. For the mouth of each estuary a roughness coefficient (k_s) was calculated based on a Chézy value of 50, 60 or 70 for small, middle and large estuaries, respectively. The roughness coefficient at the mouth (k_s) was used in the model to calculate the space- and time-varying Chézy value and drag coefficient (C_d). Friction variations along estuaries are minor and this is a common approach in numerical modelling to estimate friction[46–48]. For example, Nnafie et al.[48] use a constant Chézy value, and Geleynse et al.[46,47] use a constant Mannings value for delta branches, which only has a weak dependency on depth. Moreover, our friction assumption does not affect the main trends. Even with a perfect representation of friction (which would require grain size distributions of all estuaries, among other things), small estuaries still respond stronger to a 1-m increase in SLR than large estuaries.

Although our method to estimate tidal prism neglects tidal amplification and damping for purposes of the morphological estimation, the 1D-hydrodynamic model automatically solves amplification/damping, which was required for the effect on water levels and for our estimation of future flood risk. Implementing the tidal amplification/damping effect in the morphological estimation would require solving those two models iteratively. Because the contribution of tidal amplification/damping effect to the tidal prism is minor (10–40%), we neglect this effect for purposes of estimating morphology.

SLR scenarios. To study the effect of SLR on the future morphology and tidal range of estuaries we implemented the following scenarios (Fig. 1).

Scenario 1, a^0. An increase in MSL of 1 m in 100 years with all other boundary conditions and estuary shape remaining the same. Although precise SLR varies among systems, we used a value of 1 m, loosely based on Intergovernmental Panel on Climate Change scenarios[1,14,19], to illustrate dominant effects and response mechanisms among estuaries worldwide. For the morphological tool, a change in MSL means that all input variables remain the same and thus the estimation of equilibrium morphology is equal. This also implies that the required sediment (m^3) for morphological adaptation is equal to the estuary surface area (m^2) multiplied by the SLR (m). In the hydrodynamic model, the two extreme cases of full morphological adaptation and no morphological adaptation were calculated. In case of full morphological adaptation, the resulting tidal amplification is equal to the situation before SLR, but in the case without morphological adaptation the increased depth of channels and shoals could lead to a different degree of amplification.

Scenario 2, a^{++}, a^{+}, a^{-}. Tidal amplitude at the estuary mouth can either increase, decrease or remain constant as a result of SLR[19,20]. The two most important reasons are the shift of amphidromic points (tidal nodes) on the shelf and the reduced friction caused by an increased water depth. If the distance between the estuary mouth and the amphidromic point increases in the future, the tidal amplitude will increase, while the amplitude decreases if the distance becomes shorter[19,20]. Additionally, increased MSL may reduce friction in the coastal seas, which means tidal damping could also reduce and tidal amplitude may increase. Here we study the sensitivity of all selected estuaries to an amplitude decrease of 0.25 m (a^{-}) and an amplitude increase of 0.25 m (a^{+}) and 0.50 m (a^{++}). Changes in tidal amplitude could lead to modified equilibrium morphology and tidal amplification because they affect the tidal prism at the mouth and therefore also the channel dimensions.

Scenario 3, $W(x)^{+}$. In parallel to Room for the River projects[49] performed on Dutch rivers, we investigated whether increased space for estuaries (managed realignment) would counteract possible negative consequences of future SLR. We ran four idealized scenarios to gain an understanding of the general effects of the location of widening. In widening scenario A the mouth was widened, in

B the estuary was widened in the tide-dominated zone, in C the landward zone was widened and in D the estuary was widened by an equal distance along the full estuary (Fig. 4). In all four idealized scenarios the widening was varied between 1.05 and 5 times the original estuary area, keeping the length of the widened section constant and thus only varying local width. The idealized scenarios were applied to one large estuary (Western Scheldt in the Netherlands) and one small estuary (Dovey in Wales). The new planform was used to estimate a new morphological equilibrium, assuming that sediment from former, flooded salt marshes was entirely redistributed. This assumption is reasonable if tidal bars and salt marshes are composed mostly of sand and the contribution of mud is minor[50], which means that more sediment is needed when the subsoil is not sandy. The morphological output was subsequently input to the hydrodynamic model to calculate tidal amplification. Although we conducted model calculations for all possible ranges and combinations of future tidal amplitudes, here we isolate the effect of increased estuary planform by comparing the results to the case without changes in tidal amplitude (a^0).

Scenario 1 is predominantly used to study the effect of increased channel depth on tidal amplification. Scenario 2 reveals a relation between required sediment for adaptation and future changes in tidal range. Scenario 3 indicates whether managed realignment has the potential to mitigate adverse effects of the previous scenarios.

These scenarios simplify the morphological evolution of estuaries in the sense that we ignore the dynamic response between morphological adaptation, ebb and flood dominance and the resulting net sediment transport[40,41]. By studying the case of very rapid SLR (thus lack of time for adaptation) we manage to avoid these problems. This is no longer a situation with a subtle balance, and hence we do not calculate the evolution; nevertheless, these extreme scenarios allow us to determine qualitative trends for the fate of estuaries. What we calculate is the morphological work that needs to be done to adapt to their potential estimated equilibrium bathymetry after the rapid SLR, expressed in the amount of sediment that needs to be imported into the estuary.

Estimation of sediment balance in estuaries and reconstruction of former estuaries and deltas under SLR. To assess whether systems can keep up with future SLR, we compared the incoming fluvial sediment flux (Q_s) to the required sediment flux ($Q_{s,req}$) for a 1 m SLR in 100 years. The required sediment for this scenario was calculated as 1 m of additional accommodation space multiplied by the area of the system before SLR. We assumed that the planform of the estuary does not change and we excluded changes in tides. We also ignored that part of the required sediment for adaptation can be compensated by peat formation[51–53] or by changes in the net importing behaviour of the estuary. Peat is sensitive to salinity intrusion, which means that the estimates of required sediment are upper limits. Net sediment importing behaviour depends on asymmetry in the duration and peak velocity of ebb and flood[40,41]. Although the 1D-numerical model can provide these values (with great uncertainty because it ignores the two-dimensional nature of ebb-dominated channels and flood-dominated bars), we did not use them because the degree to which sediment can be delivered from the coast depends, among other things, on the availability of sediment at the seaward boundary. In general, it is expected that drowning estuaries become more flood-dominant and thereby import more sediment, as long as sediment is available. The actual sediment need on sediment-rich coasts may thus be lower than estimated, which again means that our estimates are upper limits.

Systematic sediment load measurements were lacking for many smaller systems and, therefore, we relied on a generic total sediment load predictor[39]:

$$Q_s = cA_{\text{catchment}}{}^{d}$$

in which Q_s is the sediment load (in million tons year^{-1}), $A_{\text{catchment}}$ is the catchment area (in 1×10^6 km^2) and c and d are parameters depending on the highest topography in the catchment (Supplementary Table 3). Catchment sizes were obtained from a geographic information system database from the US Geological Survey, which contains spatial data on catchments worldwide (https://hydrosheds.cr.usgs.gov/datadownload.php?reqdata=30bass). Topography was derived from SRTM-3 v.2 sampled at 3 arcsec.

Sediment balance for Holocene deltas and estuaries. To compare modern sediment balances to past situations, Holocene sediment balances were estimated from published geological reconstructions of several deltas and estuaries[51,54–60]. The resulting net sedimentation is a minimum value for past sediment flux, assuming maximal trapping efficiency. The difference in accommodation space between two successive time steps was calculated from relative SLR based on geological reconstructions or detailed geological profiles.

Three types of systems were distinguished: mega-deltas with ample sediment supply, peat-filled back-barriers and bay fills. For the Tokyo Bay and the Rhine Delta, data allowed comparison of a period within the mid-Holocene transgression (1–3 m per 100 years) to sediment accumulation, which is important because SLR in the twenty-second century may be equally fast[61]. For the Yellow River and Mekong mega-deltas and the filled-in Tokyo Bay (Holocene total) we artificially set accommodation space equal to stored sediment to indicate that there was no sediment shortage over the period considered.

Reporting Summary. Further information on research design is available in the Nature Research Reporting Summary linked to this article.

Data availability

All open access data are available in figures, tables and supplementary information. If used from other sources, it is indicated with references. Estuary outlines were collected from Google Earth and are available in the supplementary information of ref. [17]. Along-channel width profiles, input values to run the morphological tool and the hydrodynamic model are available from Zenodo (https://doi.org/10.5281/zenodo.3406518). Other data are provided in the figures, tables and references.

Code availability

The code for the 1D hydrodynamic model is available from Zenodo (https://doi.org/10.5281/zenodo.3406518). The code for the morphological tool has been referenced[32] and is available on GitHub (https://github.com/JasperLeuven/EstuarineMorphologyEstimator/).

References

45. Leuven, J. R. F. W., Kleinhans, M. G., Weisscher, S. A. H. & van der Vegt, M. Tidal sand bar dimensions and shapes in estuaries. *Earth Sci. Rev.* **161**, 204–233 (2016).
46. Geleynse, N. et al. Controls on river delta formation; insights from numerical modelling. *Earth Planet. Sci. Lett.* **302**, 217–226 (2011).
47. van der Wegen, M. Numerical modeling of the impact of sea-level rise on tidal basin morphodynamics. *J. Geophys. Res. Earth Surf.* **118**, 447–460 (2013).
48. Nnafie, A., van Oyen, T., de Maerschalck, B., van der Vegt, M. & van der Wegen, M. Estuarine channel evolution in response to closure of secondary basins: an observational and morphodynamic modeling study of the Western Scheldt Estuary. *J. Geophys. Res. Earth Surf.* **123**, 167–186 (2018).
49. Rijke, J., van Herk, S., Zevenbergen, C. & Ashley, R. Room for the river: delivering integrated river basin management in the Netherlands. *Int. J. River Basin Manag.* **10**, 369–382 (2012).
50. van de Lageweg, W. I., Braat, L., Parsons, D. R. & Kleinhans, M. G. Controls on mud distribution and architecture along the fluvial-to-marine transition. *Geology* **46**, 971–974 (2018).
51. Erkens, G. *Sediment Dynamics in the Rhine Catchment: Quantification of Fluvial Response to Climate Change and Human Impact*. PhD thesis, Utrecht Univ. (2009).
52. Vos, P. C. *Origin of the Dutch Coastal Landscape: Long-term Landscape Evolution of the Netherlands during the Holocene, Described and Visualized in National, Regional and Local Palaeogeographical Map Series*. PhD thesis, Utrecht Univ. (2015).
53. de Haas, T. et al. Holocene evolution of tidal systems in the Netherlands: effects of rivers, coastal boundary conditions, eco-engineering species, inherited relief and human interference. *Earth Sci. Rev.* **177**, 139–163 (2017).
54. Goodbred, S. L. Jr & Kuehl, S. A. Holocene and modern sediment budgets for the Ganges–Brahmaputra river system: evidence for highstand dispersal to flood-plain, shelf, and deep-sea depocenters. *Geology* **27**, 559–562 (1999).
55. Hori, K. et al. Sedimentary facies and Holocene progradation rates of the Changjiang (Yangtze) Delta, China. *Geomorphology* **41**, 233–248 (2001).
56. Saito, Y., Yang, Z. & Hori, K. The Huanghe (Yellow River) and Changjiang (Yangtze River) deltas: a review on their characteristics, evolution and sediment discharge during the Holocene. *Geomorphology* **41**, 219–231 (2001).
57. Ta, T. K. O. et al. Holocene delta evolution and sediment discharge of the Mekong River, southern Vietnam. *Quat. Sci. Rev.* **21**, 1807–1819 (2002).
58. Anderson, J. B., Rodriguez, A. B., Milliken, K. & Taviani, M. in *Response of Upper Gulf Coast Estuaries to Holocene Climate Change and Sea-Level Rise* Special Paper 443 (eds Anderson, J. B. & Rodriguez, A. B.) 89–104 (Geological Society of America, 2008).
59. Tanabe, S., Nakanishi, T., Ishihara, Y. & Nakashima, R. Millennial-scale stratigraphy of a tide-dominated incised valley during the last 14 kyr: spatial and quantitative reconstruction in the Tokyo lowland, central Japan. *Sedimentology* **62**, 1837–1872 (2015).
60. Koster, K., Stafleu, J. & Cohen, K. M. Generic 3D interpolation of Holocene base-level rise and provision of accommodation space, developed for the Netherlands coastal plain and infilled palaeovalleys. *Basin Res.* **29**, 775–797 (2017).

61. DeConto, R. M. & Pollard, D. Contribution of Antarctica to past and future sea-level rise. *Nature* **531**, 591–597 (2016).

Acknowledgements
This work was funded by the Netherlands Science Foundation NWO-TTW under Vici grant no. 016.140.316/13710 (to M.G.K.).

Author contributions
J.R.F.W.L., M.G.K., T.J.B. conceived and designed the study. J.R.F.W.L. and H.J.P. collected the data. J.R.F.W.L. and M.v.d.V. carried out the modelling. J.R.F.W.L. wrote the manuscript, with contributions from H.J.P., M.v.d.V., T.J.B. and M.G.K.

Competing interests
The authors declare no competing interests.

Additional information
Supplementary information is available for this paper at https://doi.org/10.1038/s41558-019-0608-4.

Correspondence and requests for materials should be addressed to J.R.F.W.L.

Reprints and permissions information is available at www.nature.com/reprints.

Peer Review Information *Nature Climate Change* thanks Erika Lentz and the other, anonymous, reviewer(s) for their contribution to the peer review of this work.

nature research

Corresponding author(s): Jasper Leuven

Last updated by author(s): Sep 12, 2019

Reporting Summary

Nature Research wishes to improve the reproducibility of the work that we publish. This form provides structure for consistency and transparency in reporting. For further information on Nature Research policies, see Authors & Referees and the Editorial Policy Checklist.

Statistics

For all statistical analyses, confirm that the following items are present in the figure legend, table legend, main text, or Methods section.

n/a	Confirmed
☒	☐ The exact sample size (*n*) for each experimental group/condition, given as a discrete number and unit of measurement
☒	☐ A statement on whether measurements were taken from distinct samples or whether the same sample was measured repeatedly
☒	☐ The statistical test(s) used AND whether they are one- or two-sided *Only common tests should be described solely by name; describe more complex techniques in the Methods section.*
☒	☐ A description of all covariates tested
☒	☐ A description of any assumptions or corrections, such as tests of normality and adjustment for multiple comparisons
☒	☐ A full description of the statistical parameters including central tendency (e.g. means) or other basic estimates (e.g. regression coefficient) AND variation (e.g. standard deviation) or associated estimates of uncertainty (e.g. confidence intervals)
☒	☐ For null hypothesis testing, the test statistic (e.g. *F*, *t*, *r*) with confidence intervals, effect sizes, degrees of freedom and *P* value noted *Give P values as exact values whenever suitable.*
☒	☐ For Bayesian analysis, information on the choice of priors and Markov chain Monte Carlo settings
☒	☐ For hierarchical and complex designs, identification of the appropriate level for tests and full reporting of outcomes
☒	☐ Estimates of effect sizes (e.g. Cohen's *d*, Pearson's *r*), indicating how they were calculated

Our web collection on statistics for biologists contains articles on many of the points above.

Software and code

Policy information about availability of computer code

Data collection	Data on estuary outlines was collected using Google Earth.
Data analysis	The code for the one-dimensional hydrodynamic model is also available via available through Zenodo (DOI: 10.5281/zenodo.3406518). The code for the morphological tool has been referenced (Leuven et al., 2018, Remote Sensing) and is available on GitHub (https://github.com/JasperLeuven/EstuarineMorphologyEstimator/).

For manuscripts utilizing custom algorithms or software that are central to the research but not yet described in published literature, software must be made available to editors/reviewers. We strongly encourage code deposition in a community repository (e.g. GitHub). See the Nature Research guidelines for submitting code & software for further information.

Data

Policy information about availability of data

All manuscripts must include a data availability statement. This statement should provide the following information, where applicable:

- Accession codes, unique identifiers, or web links for publicly available datasets
- A list of figures that have associated raw data
- A description of any restrictions on data availability

All data are open access available in the figures, tables, supplement and if used from other sources, it is indicated with references. The code for the one-dimensional hydrodynamic model is appended as Supplementary Material. The code for the morphological tool has been referenced (Leuven et al., 2018, Remote Sensing) and is available on GitHub (https://github.com/JasperLeuven/EstuarineMorphologyEstimator/). Estuary outlines were collected in Google Earth and are available as supplementary material with Leuven et al. (2018, ESPL). Along-channel width profiles, input values to run the morphological tool and hydrodynamic model are available through Zenodo (DOI: 10.5281/zenodo.3406518). Other data are given in the figures, tables and references, but are also appended an .xlsx file with all output data used to make the figures.

Field-specific reporting

Please select the one below that is the best fit for your research. If you are not sure, read the appropriate sections before making your selection.

☐ Life sciences ☐ Behavioural & social sciences ☒ Ecological, evolutionary & environmental sciences

For a reference copy of the document with all sections, see nature.com/documents/nr-reporting-summary-flat.pdf

Ecological, evolutionary & environmental sciences study design

All studies must disclose on these points even when the disclosure is negative.

Study description	We studied the effects of sea-level rise on 36 estuaries worldwide. To do so, we used a previously collected dataset with estuary outlines. On this dataset we applied a morphological tool (cited in the references) and a onedimensional hydrodynamic model (code added as supplement). Multiple scenarios were performed to assess dominant effects of sea-level rise.
Research sample	An existing dataset with estuary planforms (Leuven et al., 2018) was used and enhanced for this study. The dataset consists 36 bar filled estuaries worldwide of varying size and varying degree of tidal influence, river discharge and human influence (all listed as Suppl. Table 2).
Sampling strategy	Models were applied on an exisiting dataset. Sampling strategy is described in the original paper (Leuven et al., 2018) and was chosen such that varying sizes and varying degrees of tidal influence, river discharge and human influence are included in the dataset.
Data collection	Data were collected using Google Earth by Jasper Leuven.
Timing and spatial scale	Data were collected over the periode 2017-2018. A last check on the data was performed in December 2018 in Google Earth.
Data exclusions	We applied our analysis on an existing dataset. The selected estuaries form a representative dataset.
Reproducibility	A model approach was used. This means that results are reproducable.
Randomization	No use was made of samples/organisms/participants and/or treatments.
Blinding	Estuaries were digitised on Google Earth and scenarios were applied to all estuaries using models. No use was made of samples/ organisms/participants and/or treatments.

Did the study involve field work? ☐ Yes ☒ No

Reporting for specific materials, systems and methods

We require information from authors about some types of materials, experimental systems and methods used in many studies. Here, indicate whether each material, system or method listed is relevant to your study. If you are not sure if a list item applies to your research, read the appropriate section before selecting a response.

Materials & experimental systems

n/a	Involved in the study
☒	☐ Antibodies
☒	☐ Eukaryotic cell lines
☒	☐ Palaeontology
☒	☐ Animals and other organisms
☒	☐ Human research participants
☒	☐ Clinical data

Methods

n/a	Involved in the study
☒	☐ ChIP-seq
☒	☐ Flow cytometry
☒	☐ MRI-based neuroimaging